Nov. 25, 2014
TPF-5(264) Passive Force/Skewed Abutments
Task 11 Preliminary Report

TASK 11 REPORT

PASSIVE FORCE-DEFLECTION TESTS FOR SKEWED ABUTMENTS ON GEOSYNTHETICALLY REINFORCED SOIL

Prepared By

Kyle M. Rollins, Professor, Civil & Env. Engrg Dept., Brigham Young Univ., 368 CB, Provo, UT 84602, (801) 422-6334, rollinsk@byu.edu

Ian Oxborrow, Research Asst., Civil & Env. Engrg Dept., Brigham Young Univ., 368 CB, Provo, UT 84602; i.oxborrow@gmail.com

Kyle Smith, Research Asst., Civil & Env. Engrg Dept., Brigham Young Univ., 368 CB, Provo, UT 84602, kyle.smith@byu.net

Amy Fredrickson, Research Asst., Civil & Env. Engrg Dept., Brigham Young Univ., 368 CB, Provo, UT 84602, af711.byu@gmail.com

Arthur Guo, Research Asst., Civil & Env. Engrg Dept., Brigham Young Univ., 368 CB, Provo, UT 84602, gzifan@gmail.com

Prepared for

Research Division of the Utah Department of Transportation

Nov. 25, 2014

EXECUTIVE SUMMARY

Accounting for seismic forces and thermal expansion in bridge design requires an accurate passive force-deflection relationship for the abutment wall. Current design codes make no allowance for skew effects on passive force; however, quarter scale lab tests indicate that there is a significant reduction in peak passive force as skew angle increases for plane-strain cases in sand. This phenomenon was corroborated by large scale tests in sand. To further explore this issue, large scale field tests were conducted with skew angles of 0° and 30° with Geosynthetic Reinforced Soil (GRS) in gravel with transverse wingwalls. The abutment backwall was 11-ft (3.35-m) wide by 5.5-ft (1.68-m) high and GRS backfill consisted of densely compacted gravel with geotextile sheets at 1 ft layers. The peak passive force for the 30° skew test was found to be 63% of the peak passive force for the 0° skew case, while the predicted ratio was about 53%. These results suggest that the higher strength backfill may lead to less reduction from the skew angle effects. The passive force for the GRS backfill was actually less than the passive force for gravel alone. The increased resistance provided by shearing through the geosynethic sheets in the backfill appears to have been counterbalanced by reduced interface friction at the wall, which would lower passive resistance. No clear peak passive force occurred with horizontal deflections of 3.5 inches (9% of the wall height), but resistance continued to gradually increase. Greater movements were required to mobilize comparable resistance with the GRS backfill in comparison with the gravel backfill only. Transverse pile cap displacement also increased with skew angle and was sufficient to mobilize the frictional resistance. Heave geometries for the 0°and 30° tests were quite typically 3% to 4% of the fill height. In both cases the failure geometry extended approximately 4 ft to 6 ft (1.2 m to 1.8 m) beyond the edges of the pile cap and 10 ft to 12 (3.0 m to 3.65 m) from the face of the cap when measured perpendicular to the wall face.

INTRODUCTION

Numerous large-scale experiments have been conducted with the intent to determine the passive force-deflection curves that might be expected for dense compacted fill behind non-skewed bridge abutments (Mokwa and Duncan 2001; Rollins and Cole 2006; Rollins et al. 2010; Rollins and Sparks 2002). Much of this research indicates that the peak passive force can be accurately predicted using the log-spiral method and is achieved at a longitudinal deflection of 3% to 5% of the backwall height (Rollins and Cole 2006). Methods approximating the complete passive force-deflection curve with a hyperbola have been developed by Shamsabadi et al. (2007) and Duncan and Mokwa (2001). However, for simplicity in design, most specifications recommend a bilinear relationship (AASHTO 2011; Caltrans 2001).

Until recently, no large-scale experiments had been conducted to determine the passive force-deflection relationships for skewed bridge abutments. Furthermore, current bridge design practices assume the peak passive force is the same for skewed bridges as for non-skewed bridges (AASHTO 2011). However, field evidence clearly indicates poorer performance of skewed abutments during seismic events (Apirakyorapinit et al. 2012; Elnashai et al. 2010; Shamsabadi et al. 2006; Unjohn 2012) and distress to skewed abutments due to thermal expansion (Steinberg and Sargand 2010). Laboratory tests performed by Rollins and Jessee (2012) and numerical analyses performed reported by Shamsabadi et al. (2006) both found that there is a significant reduction in passive force as skew angle increases. Using data obtained from these studies, Rollins and Jessee (2012) proposed the correction factor, R_{skew}, given by Equation (1) which defines the ratio between the peak passive force for a skewed abutment ($P_{P\text{-}skew}$) and the peak passive force for a non-skewed abutment ($P_{P\text{-}no\ skew}$) as a function of skew angle, θ.

$$R_{skew} = P_{P-skew} / P_{P-no\ skew} = 8.0 * 10^{-5}\theta^2 - 0.018\theta + 1.0 \quad (1)$$

To more fully understand the relationship between skew angle and reduction in peak passive force, two large-scale tests were conducted to determine the passive force-deflection curves for skew angles of 0° and 30°. These tests were conducted using an existing 11-ft (3.35-m) wide by 5.5-ft (1.68-m)

high by 15-ft (4.57-m) long pile cap which has been used for a number of previously conducted lateral load and passive force-deflection tests (Rollins et al. 2010; Rollins and Sparks 2002; Strassburg 2010).

Previous tests were performed at these angles at this site with sand and gravel backfills. The two tests in this study used a GRS gravel backfill. Other passive force studies involving gravel backfill include Rollins and Cole (2006) and Pruett (2009). No other published tests involved GRS backfill, so these tests are the first of their kind. The 0° skew test for this study was conducted in a similar fashion to the tests conducted by the previous researchers. For the 30° skew test a concrete wedge was attached to the face of the existing pile cap. Testing procedures, results, comparisons to available results and recommendations based on analysis of the test results are presented in this paper.

BACKGROUND

As outlined by Burke Jr. (1994) and shown in Figure 1, the interaction of forces at the interface between the bridge abutment backwall and soil backfill may be expressed in terms of the total longitudinal force, P_L, and its components normal to and transverse to the abutment. The normal force is resisted by the passive force, P_P [see Equation (2)]; and the transverse, or shear force, P_T [see Equation (3)], is resisted by the shear resistance, P_R [see Equation (4)]. To prevent instability of the bridge caused by sliding of the abutment against the soil backfill the inequality shown in Equation (5) must be satisfied. In addition, rotation of the entire bridge can occur if the inequality in Equation (6) is not satisfied.

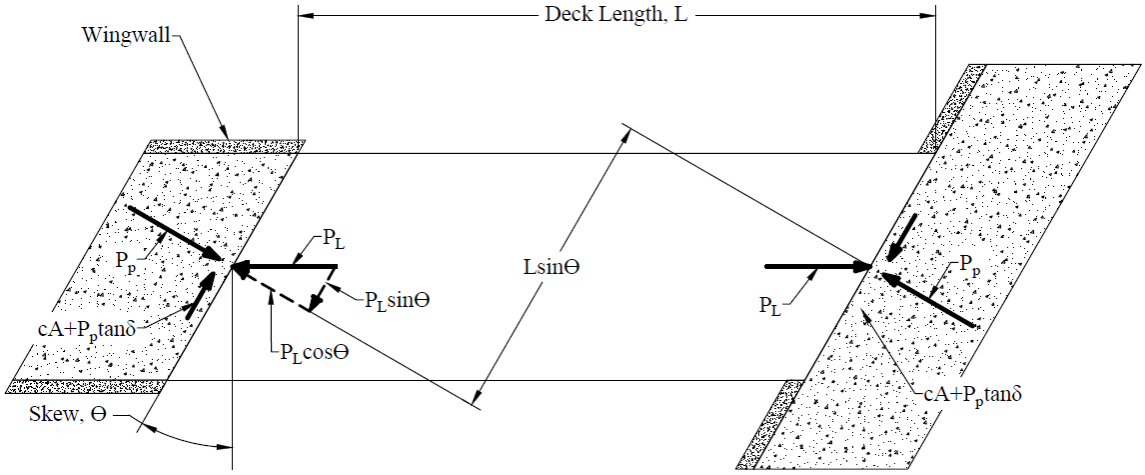

Figure 1. Typical distribution of forces on a bridge with skewed abutments.

$$P_P = P_L \cos\theta \quad (2)$$

$$P_T = P_L \sin\theta \quad (3)$$

$$P_R = cA + P_P \tan\delta \quad (4)$$

$$\frac{cA + P_P \tan\delta}{F_s} \geq P_L \sin\theta \quad (5)$$

$$\frac{(cA + P_P \tan\delta) L \cos\theta}{F_s} \geq P_P L \sin\theta \quad (6)$$

where

θ = skew angle of backwall

c = soil cohesion

A = backwall area

δ = angle of friction between backfill soil and abutment wall

F_s = factor of safety

L = length of bridge

These equations are only strictly valid if the bridge remains stable; therefore, if the bridge rotates, the distribution of forces on the abutment backwall will likely change, rendering these equations less accurate. Based on Equation (6), Burke Jr. (1994) noted that if cohesion is ignored the potential for bridge rotation is independent of passive force and bridge length so that at a typical design interface friction angle of 22°, the factor of safety decreases to below 1.5 if bridge skew exceeds 15°.

TEST CONFIGURATION

Test Geometry

The test setup for the lab tests is shown in Figure 2 and involved a 2 ft (0.61 m) high by 4 ft (1.22 m) wide backwall with a 2D or plane-strain backfill geometry (Rollins and Jessee 2012). In contrast, the field tests used an existing 11 ft (3.35 m) wide by 5.5 ft (1.68 m) high by 15 ft (4.57 m) long pile cap to simulate an abutment backwall as shown in Figure 3. Instead of a 2D backfill geometry, the backfill was

placed in a test pit that extended a little over 5 ft (1.52 m) out from the sides of the pile cap to the edge of the test pit with transverse concrete wingwalls to allow for the development of a 3D failure geometry.

The backfill was placed to 3.5 ft (1.07 m) above the base of the cap and extended 24 ft (7.32 m) longitudinally from the face of the pile cap. The backfill extended approximately 1 ft (0.30 m) below the bottom of the cap from the face to 10 ft (3.05 m) back from the face to contain the potential failure surface. Although the native soil was significantly stiffer than the backfill materials, the backfill boundaries were considered to be far enough away to not affect the development of a shear surface. Beyond 10 ft (3.05 m), the base of the backfill tapered up to be approximately even with the base of the cap to reduce the required backfill volume.

Load was applied in the longitudinal direction with two 600-kip (2,670 kN) hydraulic actuators which reacted against a sheet pile wall and two 4-ft (1.22 m) diameter drilled shafts that were coupled together by two deep beams. After conducting the test for the 0° skew conditions, two wedges, combined to create the 30° skew, were attached to the front face of the pile cap for subsequent skew tests as shown in Figure 3. Rollers were placed beneath the wedges to minimize base friction resistance.

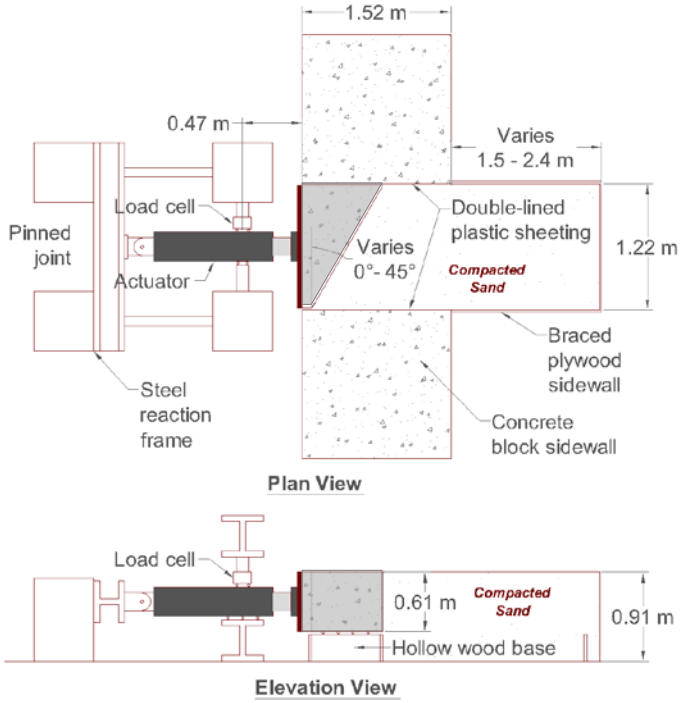

Figure 2. Schematic drawings of lab test layout (Rollins and Jessee 2012) (NOTE 1 m = 3.281 ft).

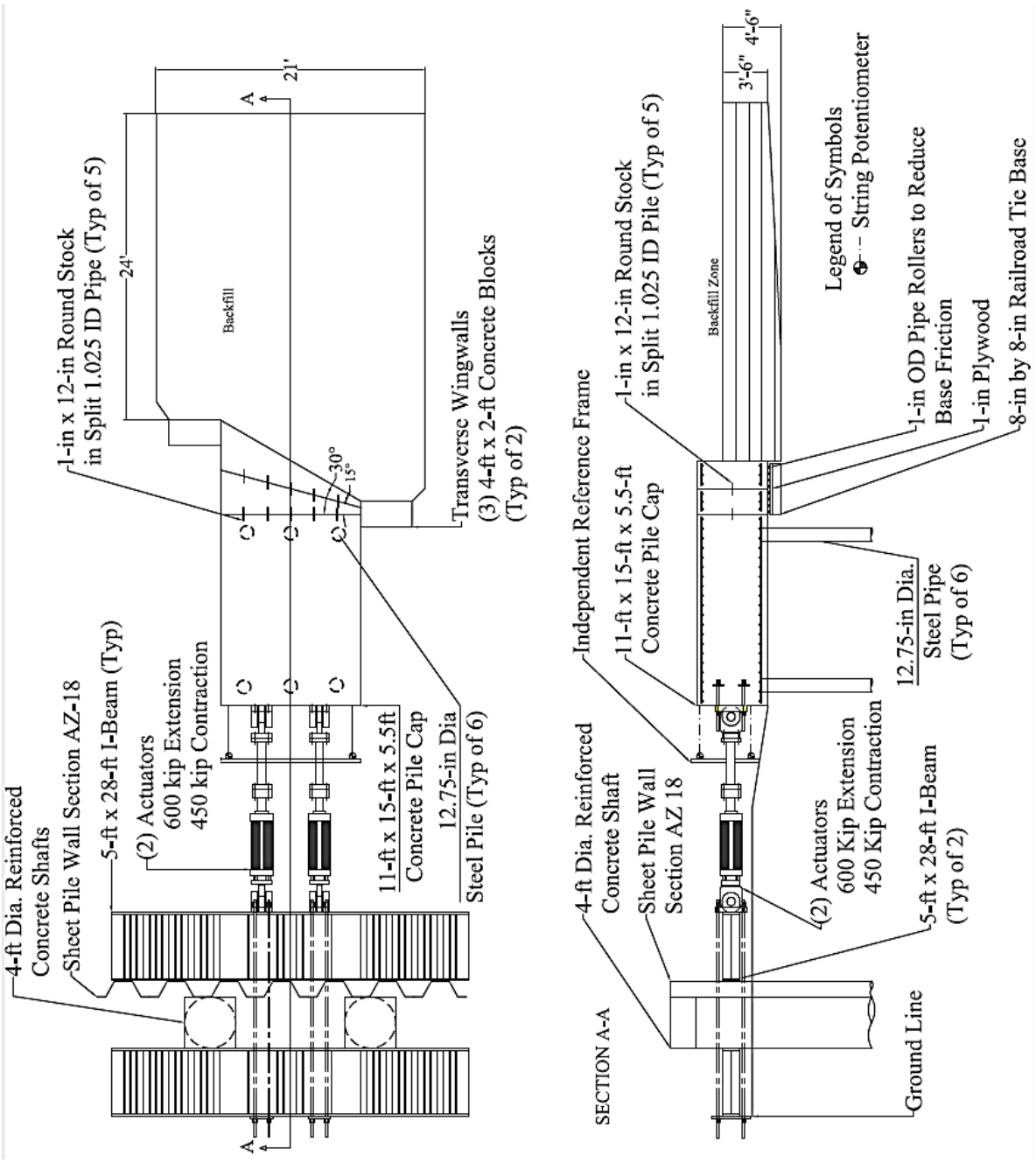

Figure 3. Schematic drawings of field test layout (NOTE 1 ft = 0.305 m).

As the backfill was placed and compacted, geotextile fabric was placed every 1 ft (0.30 m) starting at 6 in (0.15 m) below the base of the cap (see Figure 3, previous page). At each 1-ft (0.30-m) interval, the fabric extended upward along the face of the pile cap from the previous layer and was cut to a 3-ft (0.91-m) overlap then folded in over the fill before placing the new layer of fabric (see Figure 4). Therefore, the geotextile fabric was double-layered in the 3 ft (0.91-m) nearest the backwall for all intermediate layers. The resulting interface between the backfill and the backwall was completely geotextile fabric, similar to what is seen in Figure 5. The fabric was folded over in a similar fashion on the sides of the fill for the 0° skew test, layer by layer. For the 30° skew test, all layers of fabric on the sides were staked into the native soil until compaction was complete, when the stakes were removed and all the fabric layers were trimmed to a few inches above the fill. There was also a 3-ft (0.91-m) overlap between the two pieces of fabric in each layer.

Figure 4. Fabric overlap of 3 ft (0.91m) between GRS layers, 0° test. Pictured is the top of a 1-ft (0.30-m) gravel layer before the next pieces of fabric were placed for the next layer.

Figure 5. Geotextile fabric layer folds along the front of the backfill, shown by removing the west transverse wingwall after testing.

Instrumentation

Longitudinal load was measured using pressure transducers in the actuators. Longitudinal displacement of the pile cap was measured using four string potentiometers (string pots) located at each corner of the back of the pile cap and were tied to an independent reference frame. As the piles were assumed to provide vertical restraint, vertical movement of the pile cap was not monitored. Longitudinal and transverse deflection versus depth profiles were measured using inclinometers and shape accelerometer arrays (SAAs) which extended approximately 40 ft (14 m) into the center pile in the North and South sides of the pile cap. The shape arrays provided data at 1 ft (0.30 m) intervals while the inclinometers provided data at 2 ft (0.6 m) intervals. Because of the time required to obtain inclinometer readings, the inclinometer measurements were only taken immediately before the start of a test and after the last deflection increment. In contrast, the shape arrays provided profiles at each deflection increment because their collection was instantaneous.

To measure backfill heave and displacement, a 2 ft (0.61 m) grid was painted on the backfill surface and the relative elevation of each grid intersection was measured with a survey level and total station prior to and after conducting each test. Surface cracks in the backfill were also marked following the completion of each test.

Geotechnical Backfill Properties

Backfill material consisted of a well-graded gravel with silt and sand (GW-GM as classified by the Unified Soil Classification System or A-1-a according to the AASHTO classification system). Results from two gradation tests on the backfill performed by the supplier and one performed at the BYU Soil Mechanics lab are shown in Figure 6. The particle-size distribution curves generally fall within the gradation bounds specified for these GRS tests. They also correlate well to the dense coarse gravel backfill used by Rollins and Cole (2006), though with significantly less gravel and more fines than the backfill used by Pruett (2009).

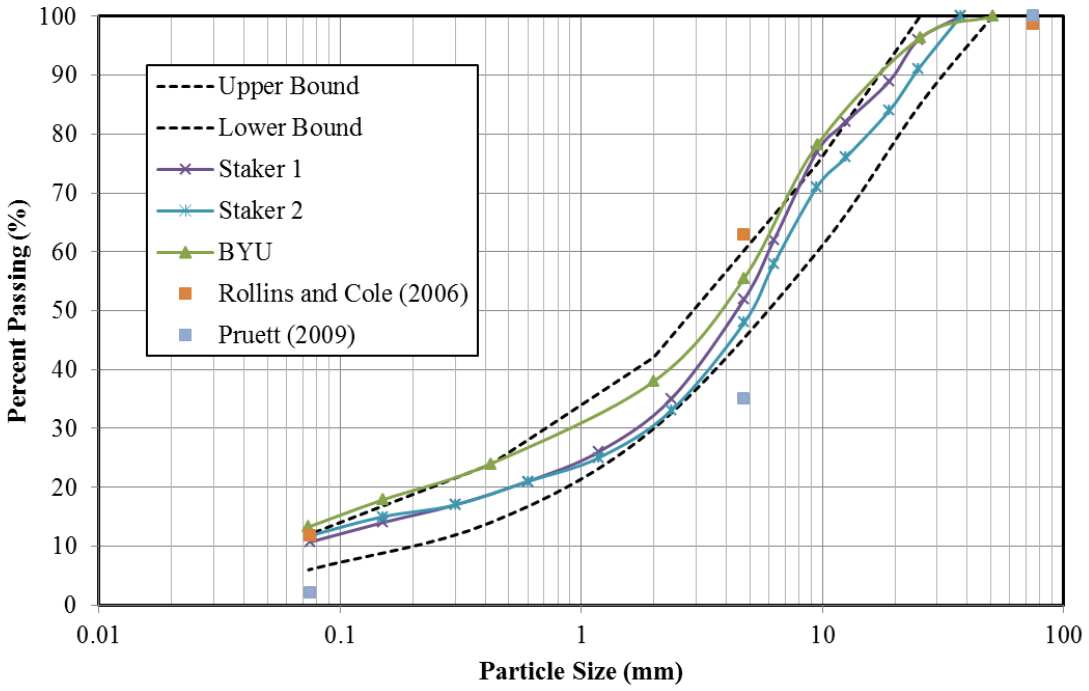

Figure 6. Gradation for backfill sand relative to concrete sand gradation.

Unit Weight and Moisture Content

Maximum dry unit weight according to the modified Proctor compaction test (ASTM D1557) performed prior to testing was 142.0 lb/ft^3 (22.3 kN/m^3) and the optimum moisture content was 6.3%. The target on-site compaction level was 95% of the modified Proctor maximum. Backfill gravel was placed in lifts approximately 4- to 6-in (15.24-cm) thick and compacted with a smooth-drum vibratory roller and a walk-behind vibratory plate compactor to an average density greater than approximately 95% of the modified Proctor maximum. A nuclear density gauge was used to obtain relative compaction and water content data during compaction. The measured dry unit weight and moisture content versus depth for the zero skew test are provided in Figures 7 and 8, while similar plots for the 30º skew are provided in Figure 9 and 10. Though not shown, the variation of relative compaction was not significant. Relative density was estimated using the empirical relationship between relative density (D_r) and relative compaction (R) for granular materials developed by Lee and Singh (1971) as shown in Equation (7) where D_r and R are measured in percent.

$$R = 80 + 0.2D_r \quad (7)$$

A summary of the backfill unit weight and water content measurements for the two tests is shown in Table 1. The properties of the two backfills were generally very consistent. Average relative compaction, relative density, and water content for the two tests were 96.2%, 82.75%, and 6.2%, respectively.

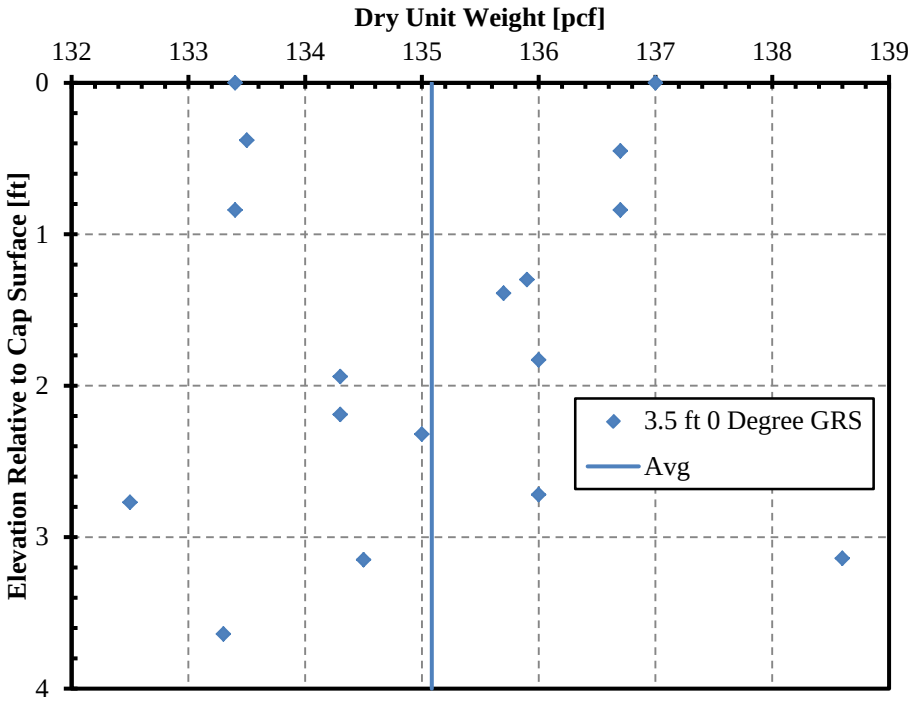

Figure 7. Dry unit weights for 0° skew

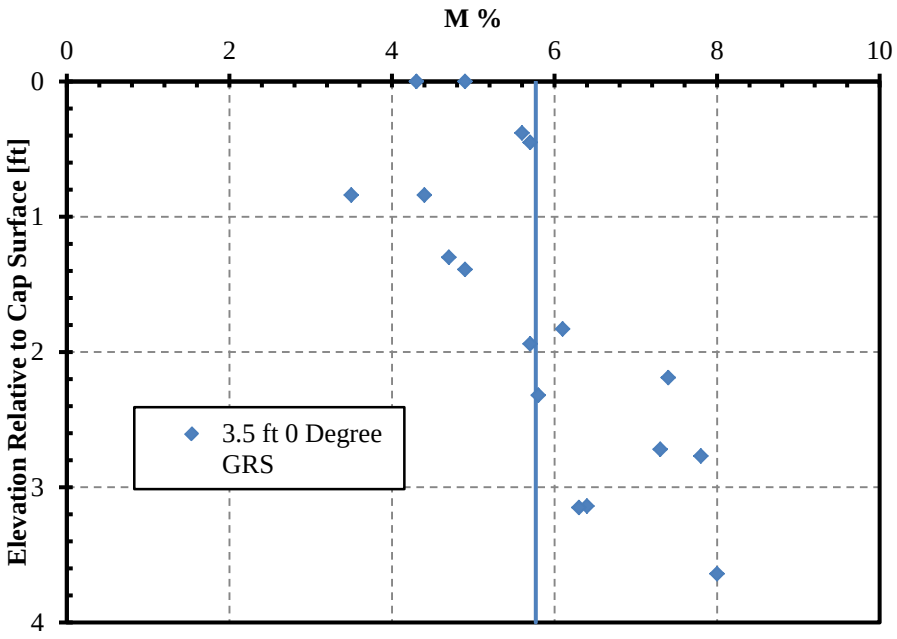

Figure 8. Moisture contents for 0° skew

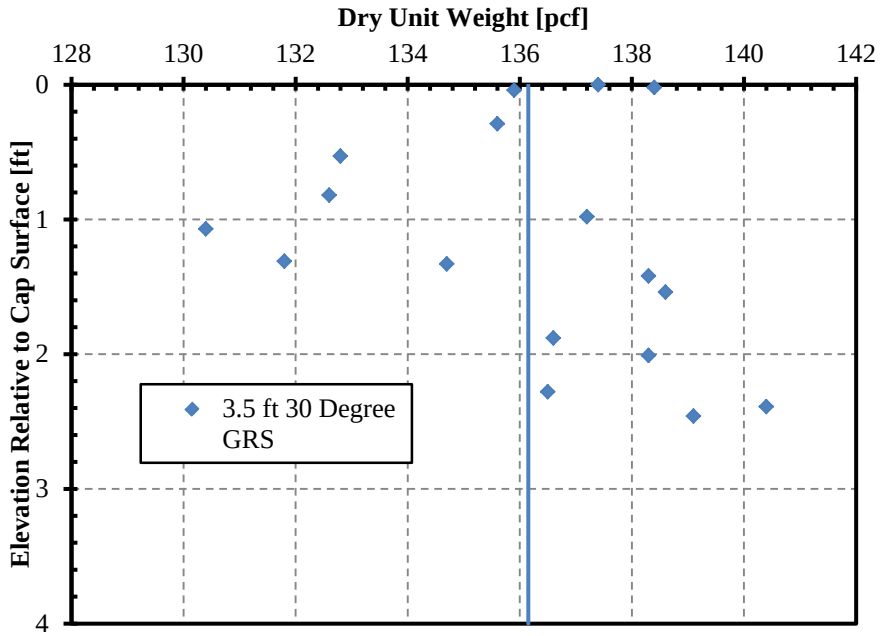

Figure 9. Dry unit weights for 30° skew

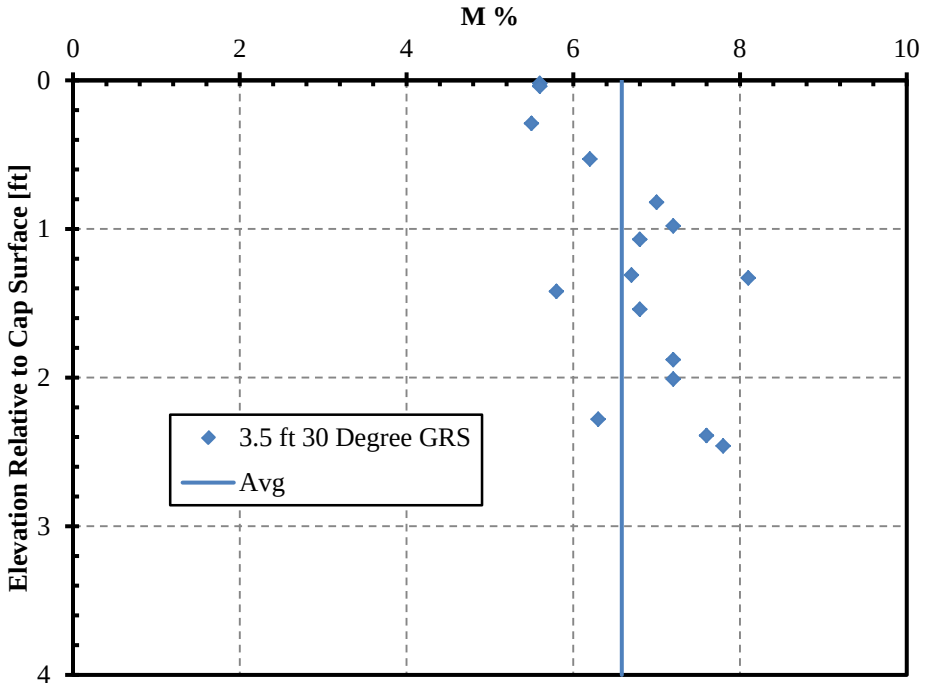

Figure 10. Moisture contents for 30° skew

Table 1. Summary of Compaction and Water Content Data for Each Test

Backfill Soil Properties	**0º Skew Test**	**30º Skew Test**
Minimum Dry Unit Weight [pcf]	132.5	130.4
Maximum Dry Unit Weight [pcf]	138.6	140.4
Average Dry Unit Weight [pcf]	135.1	136.2
Relative Compaction	96.2%	96.9%
Relative Density	81%	84.5%
Moisture Content	5.8%	6.6%

Shear Strength

In situ direct shear tests were conducted for the gravel backfill without geotextile. Figure 11 shows photo of the shear tests being performed. The tests were performed after the non-skewed 3.5 ft unconfined gravel test, which had been compacted at 96.2% maximum density. The box was carefully lowered into place by chipping away the soil around the box and tapping the box downward, into the backfill. Once in place, weights were loaded on top of the soil and a hydraulic jack was used to apply the lateral force. Displacement was measured with a dial gauge.

Two separate in situ tests were performed and the results are shown in Figure 12. The drained friction angle (ϕ') was found to be 45.8° with a cohesion of 40 lbs/ft^2 (6.3 kN/m^2). Previous researchers (Rollins and Cole 2006) conducted direct shear tests and determined that the interface friction angle (δ) between similar coarse gravel soil and concrete was about 75% of the soil friction angle. However, with the geotextile wrapped around the soil on the side of the pile cap, there was no soil-concrete interface. Instead, there was a soil-fabric interface and a fabric-concrete interface. The bulk of the movement and, therefore, the resistance likely would have been along the fabric-concrete interface.

Figure 11. Photo of in-situ direct shear test on gravel backfill

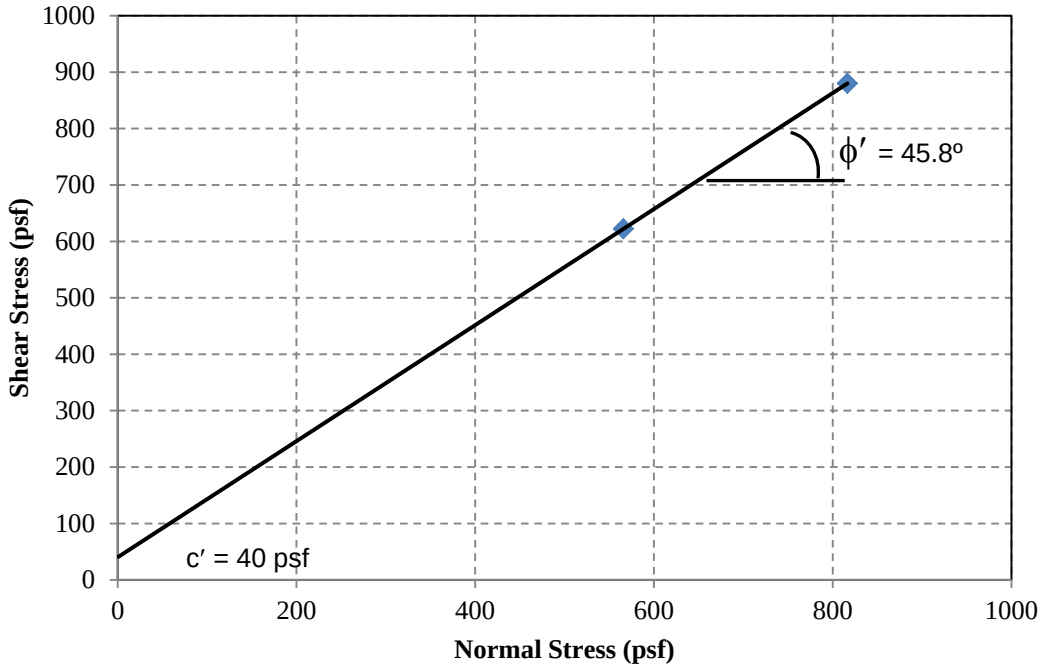

Figure 12. In situ direct shear results for gravel backfill

Geosynthetic Fabric Properties

The geotextile sheet used for the GRS tests was Mirafi® RS380*i* which was donated by Tencate Geosynthetics Americas for this research project. This geotextile is woven from polypropylene filaments to provide desired strength and soil retention characteristics along with high water flow capacity. Based on test results from the manufacturer, the geotextile has a tensile modulus of 51,000 lbs/ft, which equates to a tensile strength of 2550 lbs/ft at a strain of 5%. The geotextile has an apparent opening size (AOS) equivalent to a #40 U.S. sieve size (0.43 mm). The pore sizes for O_{95} and O_{50} are 365 and 185 microns, respectively. Permittivity is 0.9/sec and flow rate is 75 gal/min/ft^2. The interface coefficient for sand and gravel is 0.89. A photograph of the woven fabric is provided in Figure 13.

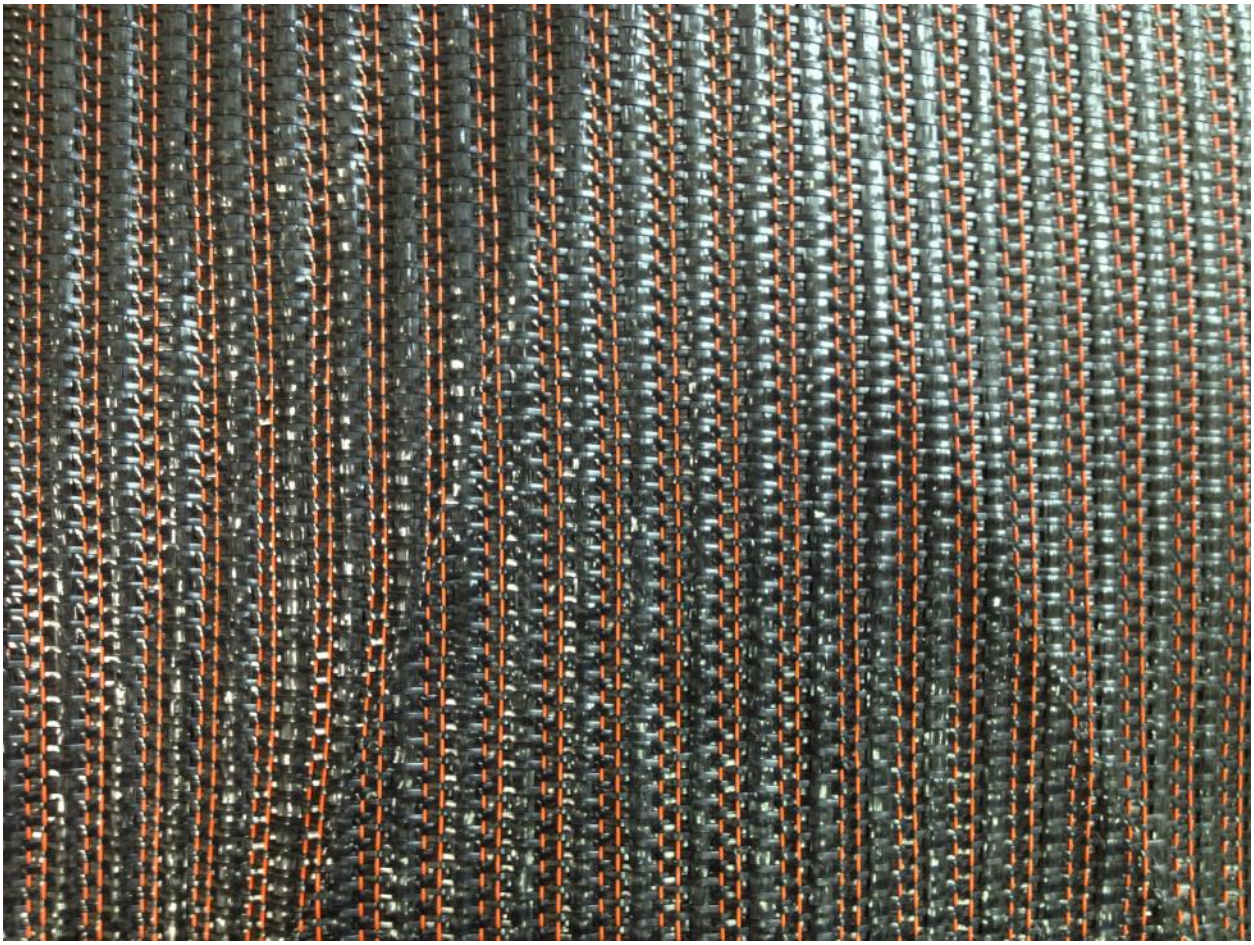

Figure 13. Photograph of the Mirafi® RS380*i* which was donated by Tencate Geosynthetics Americas for use in this GRS research study.

General Test Procedures

Prior to testing with the backfill in place, a lateral load test was performed to determine the "baseline" resistance of the pile cap alone, and the pile cap with attached 30° wedge. Because the pile cap had been previously employed for a number of tests, the baseline resistance has become relatively linear. Following the baseline test, backfill was compacted adjacent to the cap with fabric layers placed and a lateral load test was performed to obtain the total resistance. Following backfill compaction, the reference grid was painted and appropriate initial measurements, including relative elevations of the grid points, were recorded. The backfill material was completely excavated and re-compacted for each individual test. New reinforcement fabric was also placed for each test.

The pile cap (and attached wedge if applicable) was then pushed longitudinally into the backfill zone in 0.25-in (6.35-mm) increments at a velocity of 0.25 in/min (6.35 mm/min) to a final displacement of 3.5 in to 3.75 in (8.30 cm to 9.53 cm) using the two hydraulic actuators. At each 0.25-in (6.35-mm) displacement increment the load was held for approximately 2 minutes to observe the reduction in longitudinal force against the backwall as a function of time. On average, the reduction in force after 2 minutes was 9%.

Plots of the total load and corresponding baseline curve for the 0° and 30° skew tests are shown in Figure 14 and Figure 15, respectively. The resistance of the pile cap in the longitudinal direction is made up of both the passive and shear resistance of the pile cap. This resistance is represented by the difference between the total and baseline curves.

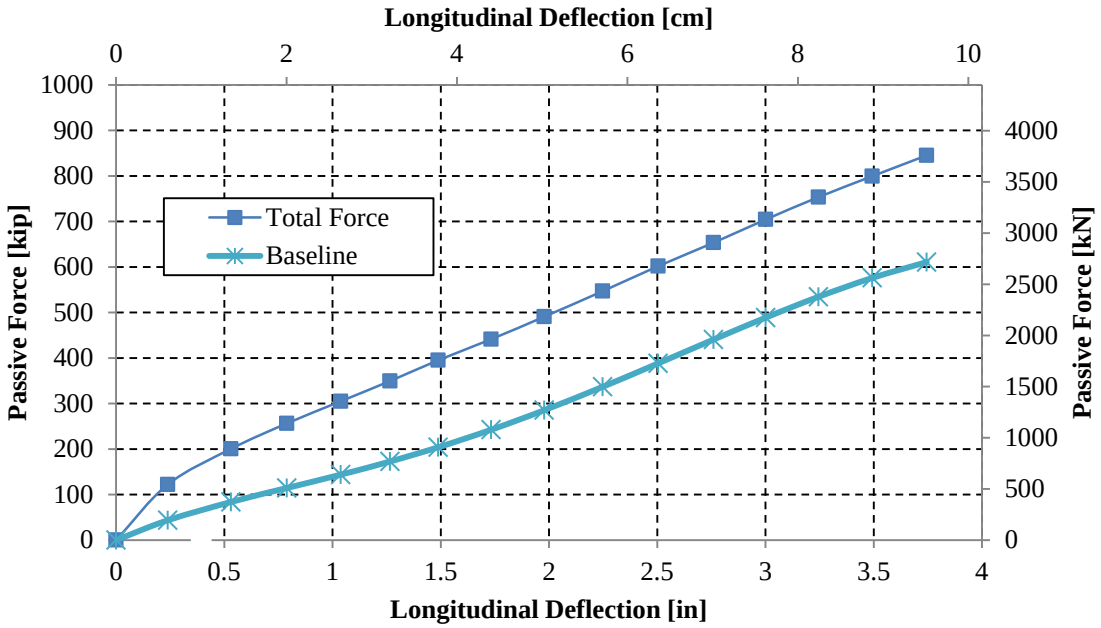

Figure 14 Total force and baseline resistance for 0° skew test.

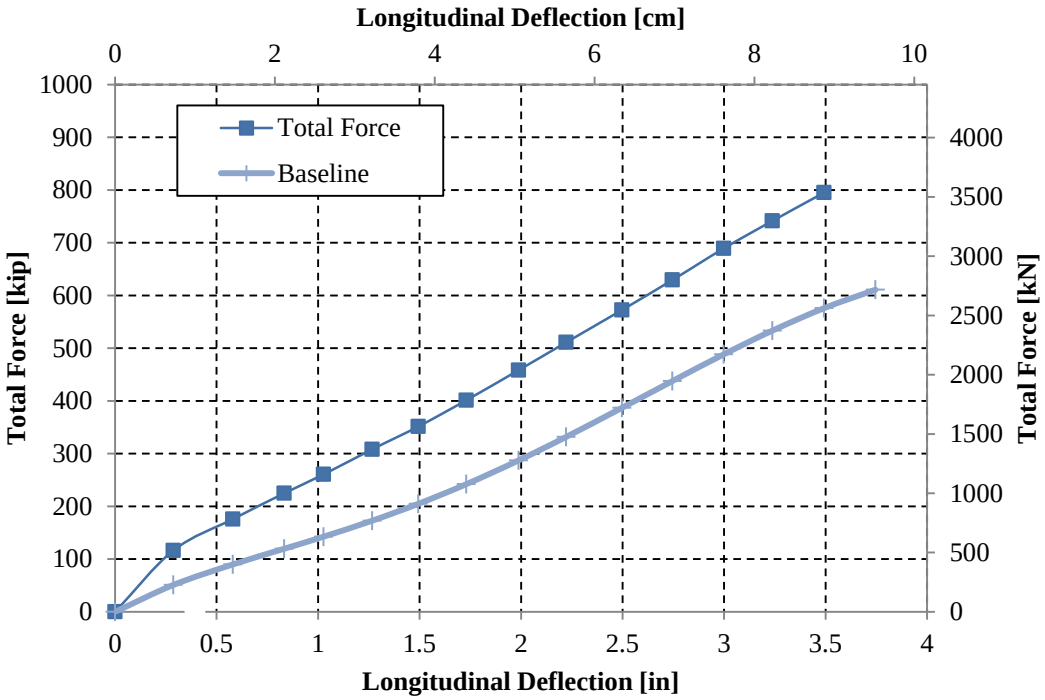

Figure 15 Total force and baseline resistance for 30° skew test.

TEST RESULTS

Passive Force-Deflection Curves

Figure 16 shows the total force versus longitudinal deflection curves for the 0° and 30° skew field tests. Passive force was calculated from the total actuator load corrected for the appropriate baseline curve using Equation (2). Backwall deflection was computed as the average deflection of the four string pots on the back of the pile cap. For both tests, the peak passive force does not reach a clear peak even at displacements as high as 3.5 inches. Although the rate of increase in resistance decreases, there is still a gradual increase in resistance with displacement for normalized displacements up to 9% of the wall height. In contrast, most tests on solely soil backfill reach a peak resistance at deflections between about 0.03H and 0.06H. Perhaps additional movement is required to fully mobilize the resistance provided by the geosynthetic sheets.

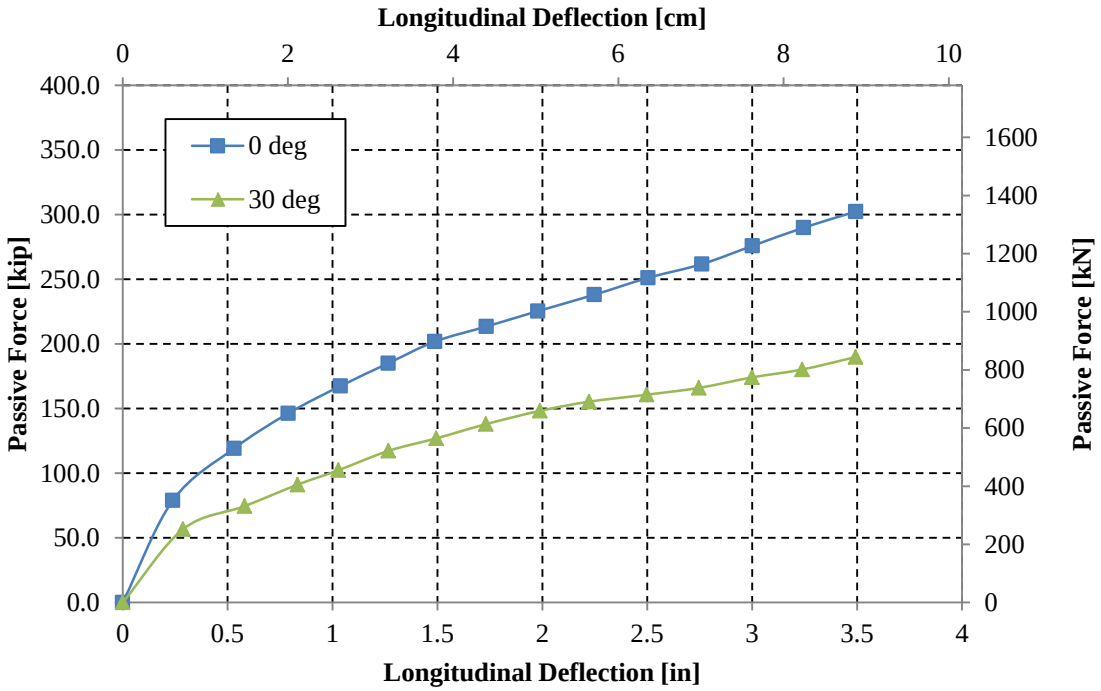

Figure 16. Comparison of passive force versus longitudinal deflection curves for 0° and 30° skew angles

Figure 17 plots the passive force reduction factor versus skew angle obtained from these tests in comparison with the lab tests conducted by Rollins and Jessee (2012) and the numerical models reported by Shamsabadi et al. (2006). As can be seen from Figure 17, Equation (1) predicts that at a 30° skew angle the passive force reduction factor should be 53% when compared to the 0° skew case. The measured reduction value was actually 63% however; this value is only slightly higher than for the case where the backfill consisted only of gravel (58%). These results suggest that the reduction factor might be somewhat higher for gravel than for sands.

The passive resistance for a backfill with layers of geosynthetic sheets would be expected to be larger than for a backfill of soil only because the shear plane would be expected to pass through each textile layer. However, this was not the case for this set of tests. The passive force for the 0º and 30º skew GRS tests were only 86% and 94%, respectively, of the resistance provided by the comparable tests with gravel backfill only as shown in Figure 18. In addition, more much more deflection was required to develop resistance for the GRS back than the gravel backfill. Of the possible explanations for the reduced resistance in both these GRS tests, one major consideration is the possibility that the friction between the concrete and the fabric is lower than the friction between the concrete and the soil. Because the ultimate passive force is highly dependent on the interface friction on the wall, a decrease in wall friction would likely lead to a significant reduction in passive force. Although the geotextile might have increased the passive resistance as the shear surface moved through the backfill, the reduction in the wall friction might have ultimately decreased the resistance.

Additionally, GRS becomes more beneficial as confining pressures increase; however in the relatively shallow depth of soil directly behind a bridge abutment, those confining pressures may be relatively small. Therefore, the fabric in the GRS may not contribute to the extent desired. Lastly, it is possible that bending of the geosynthetic sheets may occur as the shear plane intersect the sheets and movement at the intersection may be insufficient to fully mobilize the tensile resistance of the fabric. Other factors may apply, but these three mechanisms appear to be reasonable causes for the observed variation.

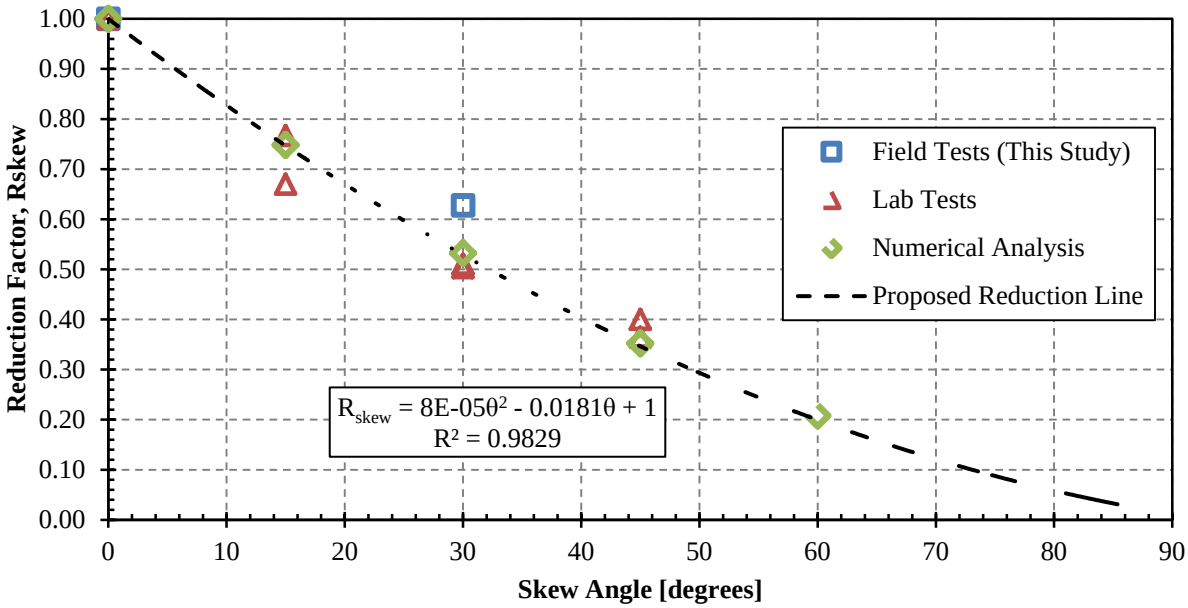

Figure 17. Reduction factor, R_{skew} (passive force for a given skew angle normalized by passive force with no skew) plotted versus skew angle based on lab tests (Rollins and Jessee 2012), numerical analyses (Shamsabadi et al. 2006), and results from field tests in this study.

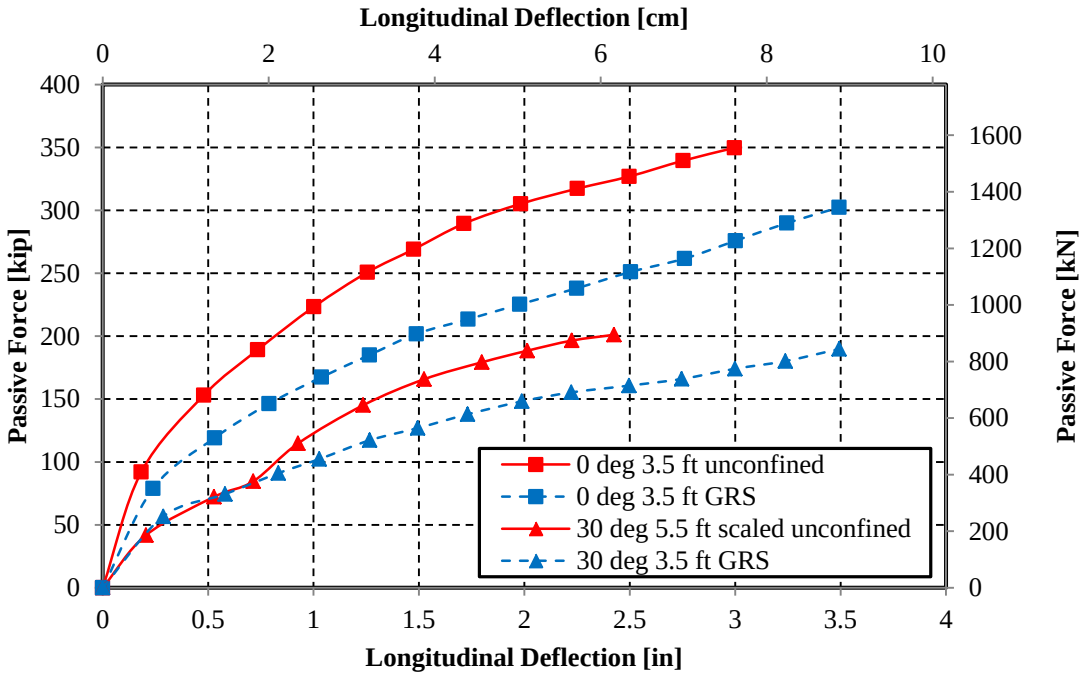

Figure 18. Comparison of passive force versus longitudinal deflection curves for unconfined gravel and gravel GRS tests.

Pile Cap Displacement vs. Depth

Figure 19 and Figure 20 provide longitudinal deflection versus depth profiles obtained from both an inclinometer and an SAA for the non-skewed test and the 30° skew test, respectively. Both profiles represent pile cap behavior for the final longitudinal displacement of the test. The depths are referenced to the top of the cap. The average deflection measured by the string pots at two elevations on the pile cap are also shown for comparison purposes. The graphs demonstrate that the measurements for the three systems were reasonably consistent and aligned with each other. For the non-skewed test, the percent difference between the north inclinometer and shape array profiles from the top of the cap to a depth of 15 ft (4.6 m) ranged between 0.6 and 12.7% with an average of 4.3%. For the 30° skewed test, the percent difference between the north inclinometer and shape array profiles from the top of the cap to a depth of 15 ft (4.6 m) ranged between 0.9 and 7.7% with an average of 3.8%. The displacements below a depth of 15 ft (4.6 m) were 0.05 in (0.13 cm) or less and the error values in this zone are not particularly meaningful.

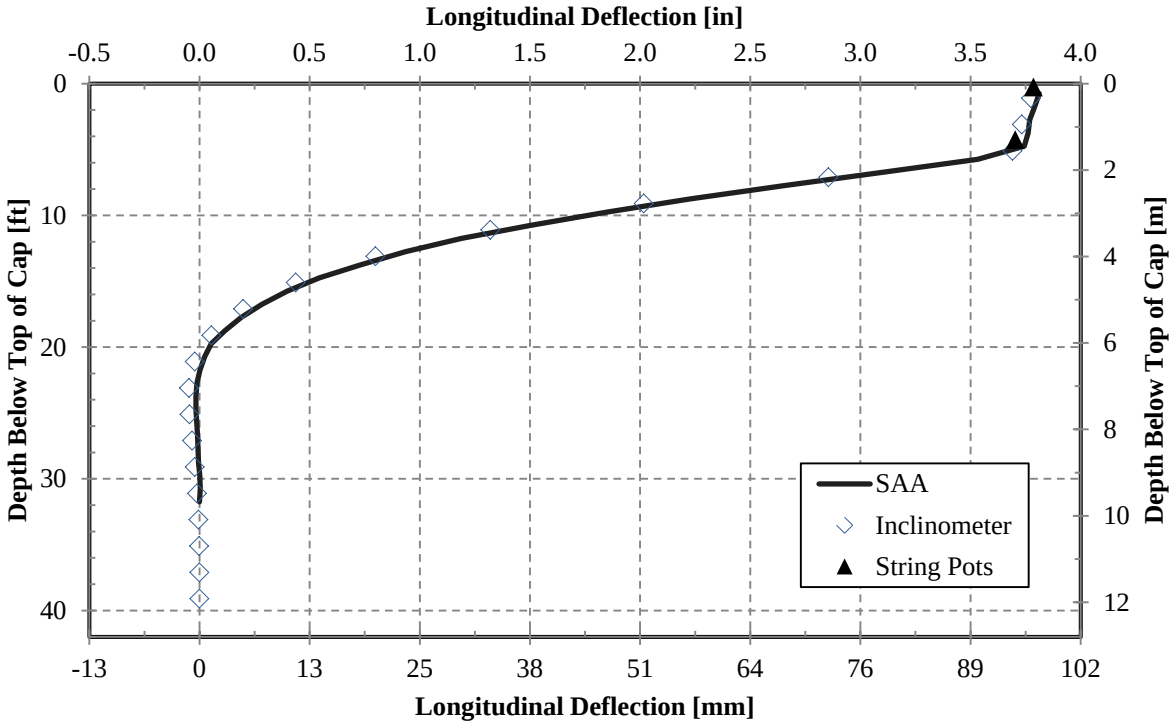

Figure 19. North 3.5-ft GRS gravel backfill 0° skew final deflection comparing inclinometer, shape array, and string potentiometers

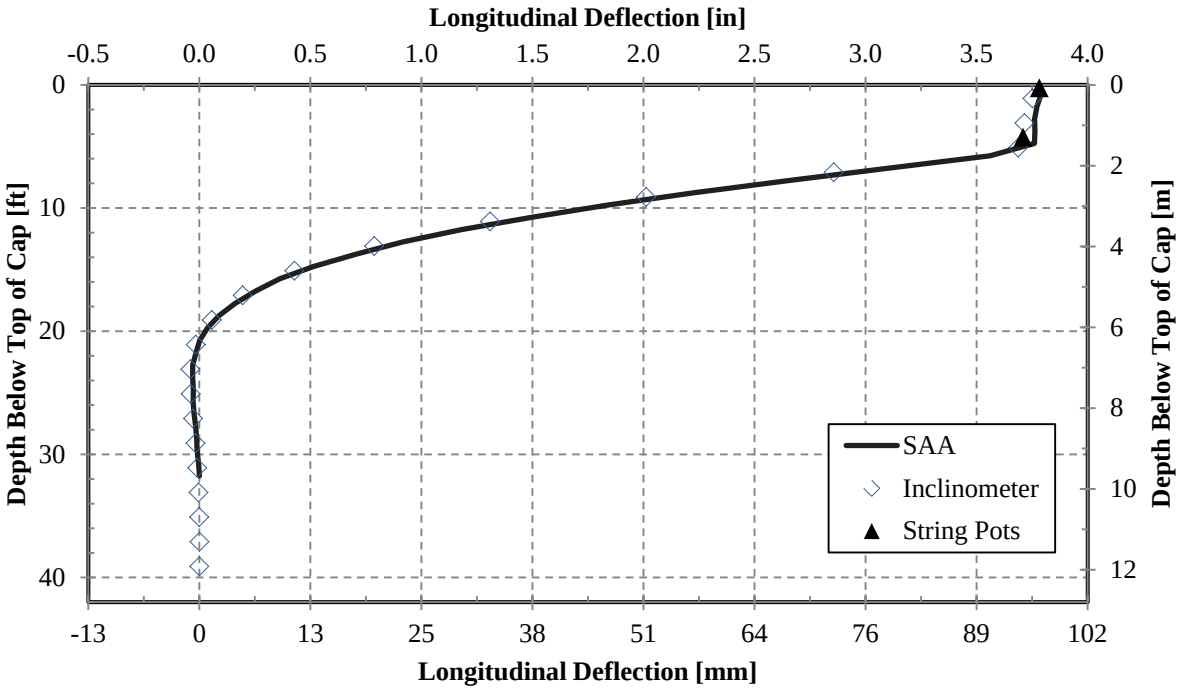

Figure 20. North 3.5-ft GRS gravel backfill 30° skew final deflection comparing inclinometer, shape array, and string potentiometers

The measurements indicate a relatively linear deflection profile within the pile cap and small cap rotations. Below the base of the cap, the piles deflect in a non-linear fashion with the deflections reaching a point of counterflexture at depth of approximately 21 ft (6.3 m) and a point of fixity at about 31 ft (9.45 m). Agreement between the north and south inclinometers was generally very good.

Transverse deflection versus depth profiles for the pile cap, also recorded by shape array and inclinometer, are plotted in Figure 21. Plotted on a smaller scale, the percent error seems larger than the longitudinal error although the magnitude difference is small. However, as observed for the deflections below 15 ft (4.6 m) in the longitudinal test, the percent difference is exaggerated due to the smaller scale. The percent difference is within the error thresholds of each instrument ($\pm$1.5 mm/30 m for shape array, and $\pm$1.24 mm/30m for inclinometer) (Rollins et al.

2009). Once again, the shape of the deflection profile indicates essentially linear deflection in the pile cap and very small rotations. The deflection in the piles is non-linear and decreases to zero at a deflection of about 30 ft (9 m).

Although the inclinometer readings were only taken at the maximum deflection for each load test, shape array profiles in the longitudinal and transverse directions were obtained at each deflection increment for each test. Figure 23 and Figure 24 show profiles of longitudinal deflection vs. depth for each deflection increment. As the deflection level increases the deflection of the pile cap remains linear but the rotation progressively increases while the depth to the point of fixity increases. Similar curves were obtained in the transverse direction.

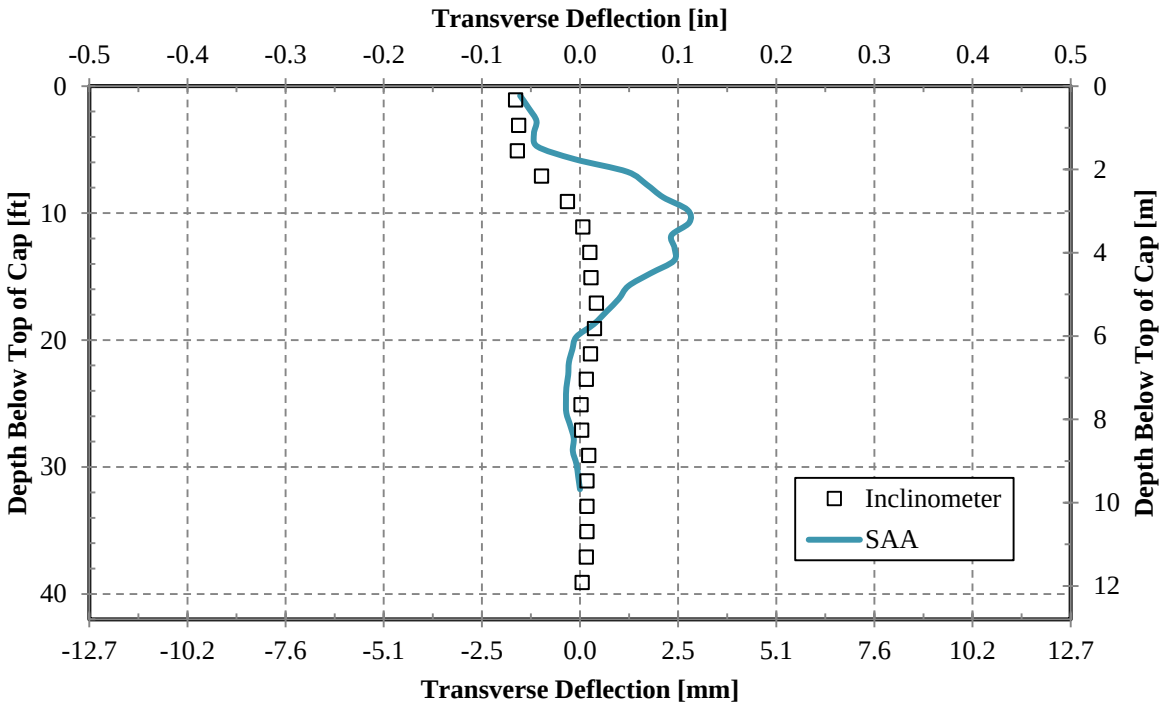

Figure 21. North 3.5-ft GRS gravel backfill 0° skew final deflections comparing inclinometer and shape array

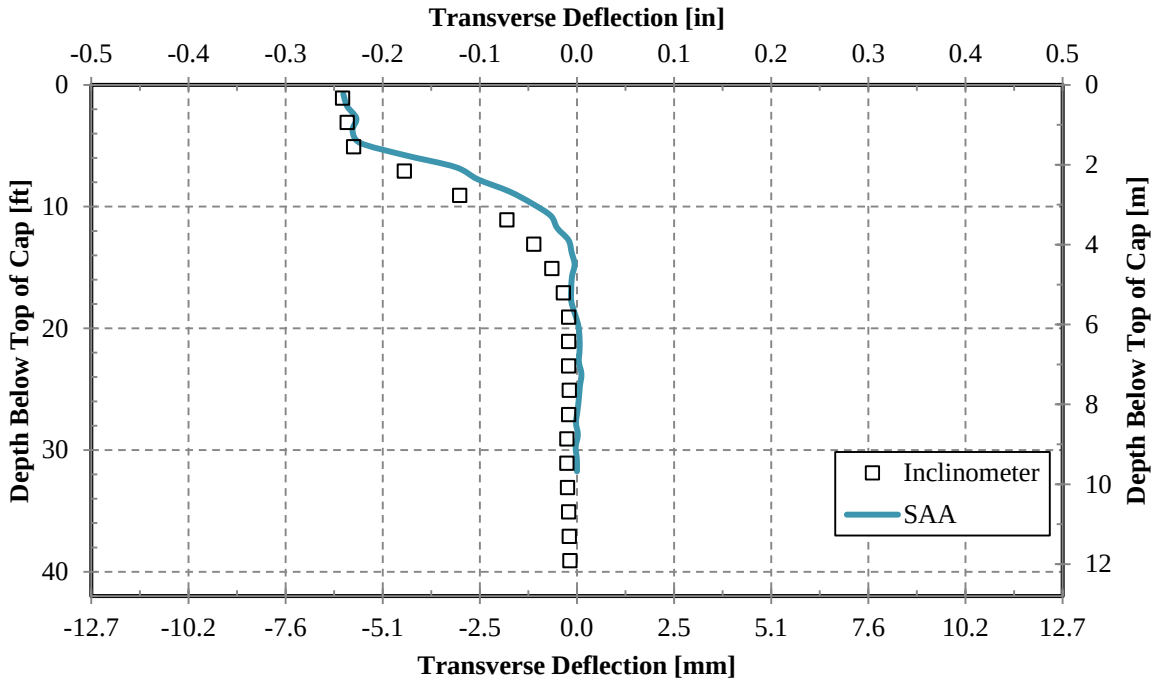

Figure 22. North 3.5-ft GRS gravel backfill 30° skew final deflections comparing inclinometer and shape array

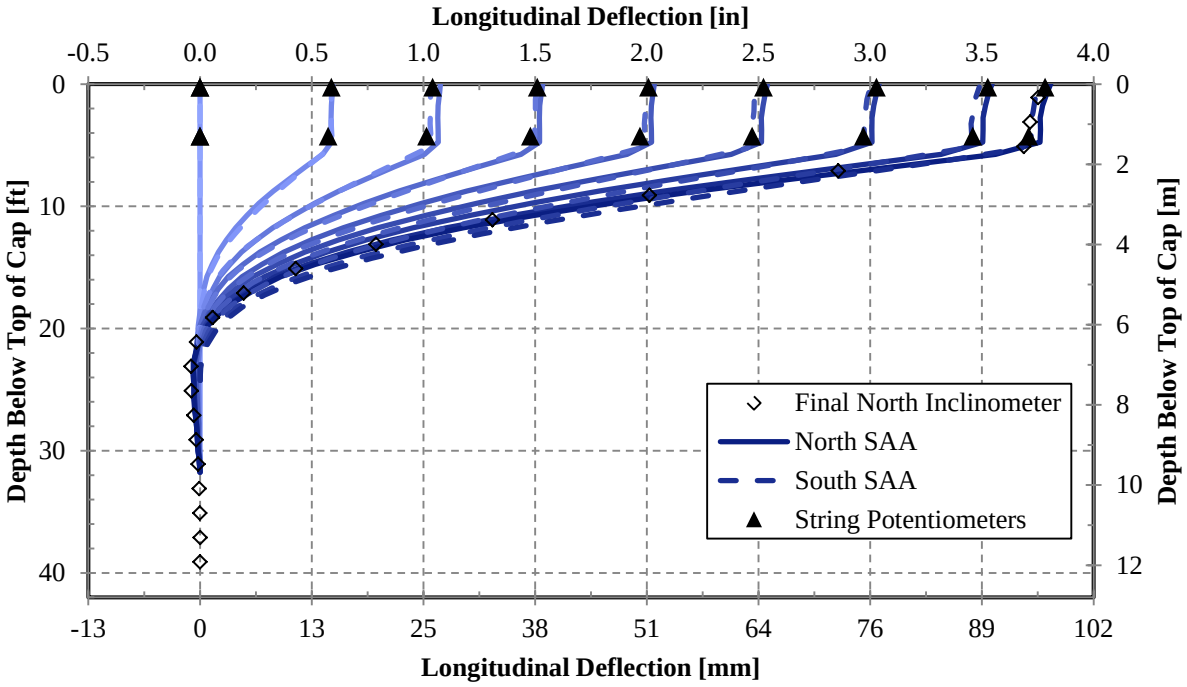

Figure 23. Longitudinal deflection vs. depth curves from SAA and string potentiometer data at various deflection increments for 0° skew Test

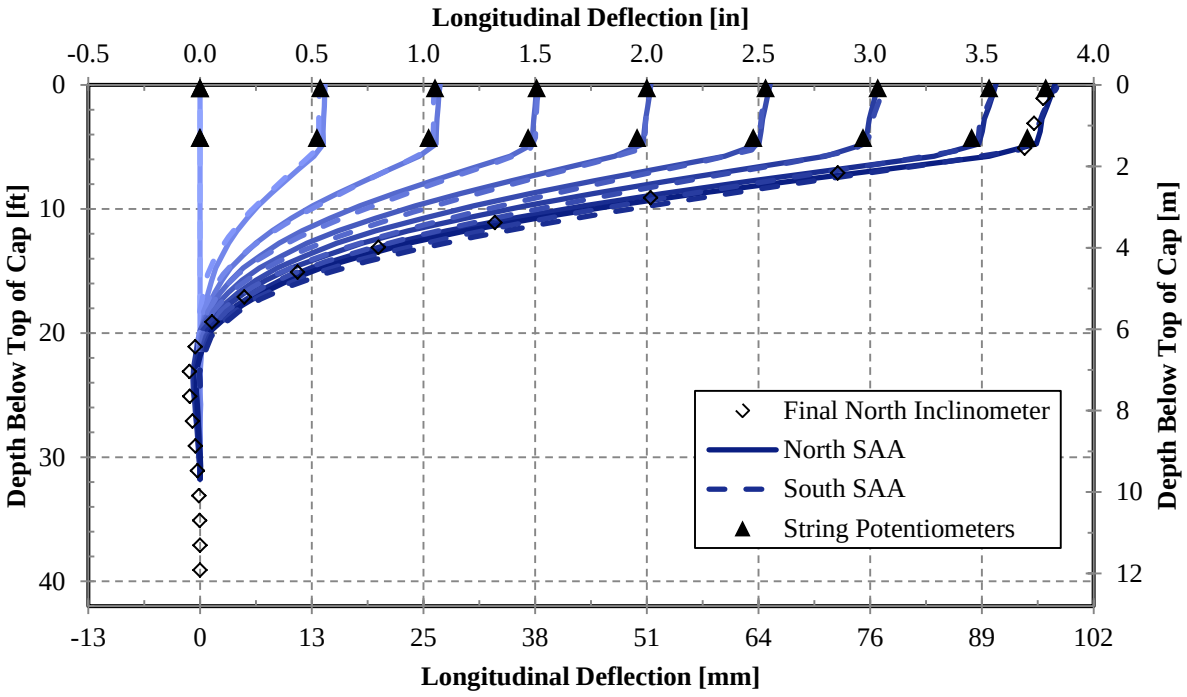

Figure 24. Longitudinal deflection vs. depth curves from SAA and string potentiometer data at various deflection increments for 30° skew Test

As noted previously, the inclinometer and shape arrays measured transverse deflections for the north and south sides of the pile cap with depth. The measured transverse deflections at the top of pile cap on both the north and south sides of the cap after the last deflection increment for each test are plotted in Figure 25 from a plan view perspective. By connecting these points on the north and south sides, the rotation of the cap can be visualized. Although deflections of both actuators were kept relatively constant throughout the test, rotation and transverse deflection were still affected by the skew angle. As seen in Figure 25, for both the 0° and 30° skews the pile cap ultimately shifted to the left (the direction of the skew) by approximately 0.04 and 0.21 inch, respectively. Both rotated approximately 0.02° in the counter-clockwise direction.

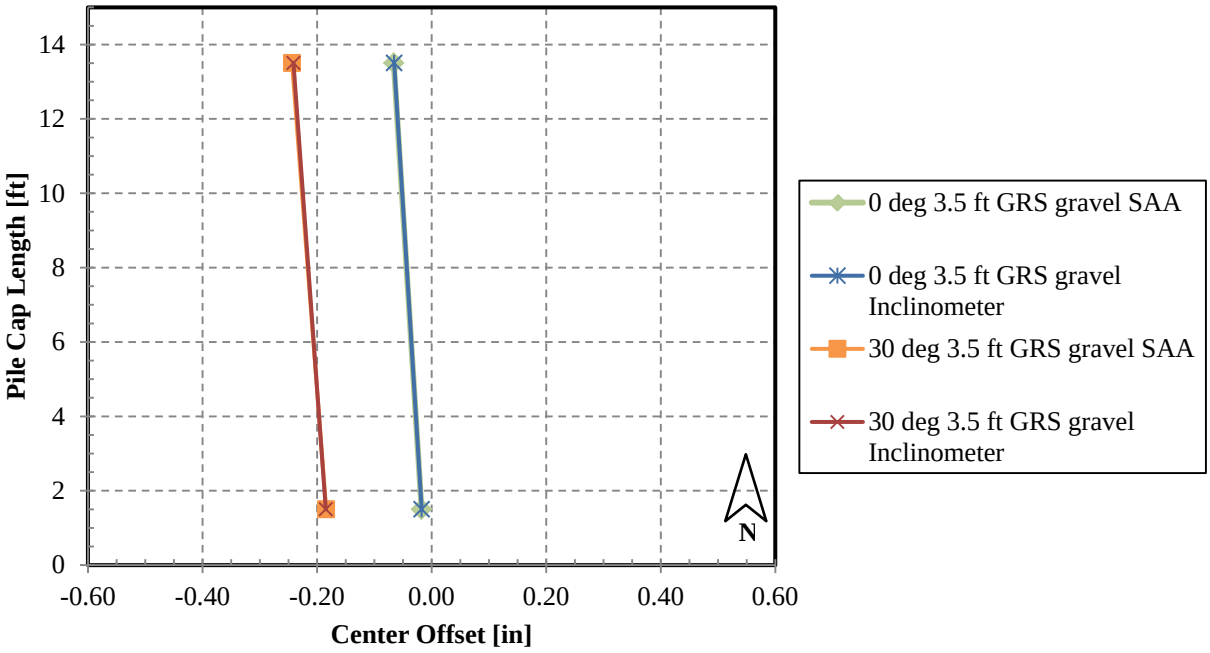

Figure 25. Transverse pile cap deflection and rotation determined between north and south shape array and inclinometer data

Applied Shear Force vs. Transverse Displacement

The relationship between the applied shear force (P_T) and transverse displacement for both the GRS gravel test and the unconfined gravel test at 30° is plotted in Figure 26. The applied shear force was computed using Equation (4) and displacement values were based on shape array measurements taken during testing. The two curves are nearly identical suggesting that lateral response is similar for both cases.

In Figure 26 B the shear force for each cap has been normalized by the maximum shear force. The maximum shear force occurred at the maximum longitudinal force. The shear force in both cases is accommodated with a displacement of about 0.3 inches. Frictional resistance along the back face of the pile cap would have been expected to develop at this deflection level.

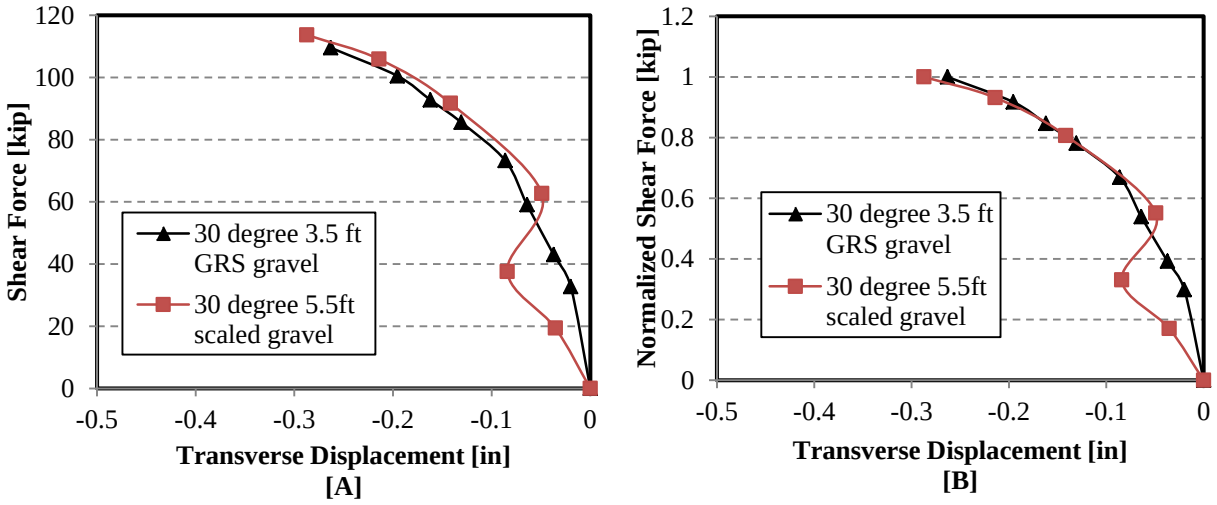

Figure 26. [A] Applied shear force versus transverse displacement; [B] Normalized applied shear force versus transverse displacement

Failure Surface Geometry

Backfill heave contours and surface cracks for the non-skewed and 30° skewed abutments are illustrated in Figure 27 and Figure 28. Heave contours for the non-skewed abutment have generally been symmetrical in other non-skewed tests; however, in this case, the heave was 1.0 in (2.5 cm) greater behind the east side of the backwall relative to the west side. One potential cause for this asymmetry is the placement of the 2-ft wide pre-cast block wingwall on the east side of the wall to accommodate a reaction wall for transverse load testing. The heave contours are also higher on the east side for the 0° skew test with gravel backfill when this same wingwall geometry was used (see Task Report 10, Fig. 23). The maximum heave (4.9 in or 12.4 cm) occurred near the east abutment edge, 1 ft (0.30 m) from the backwall. Surface cracks typically developed about 6 to 8 ft (1.8 to 2.4 m) longitudinally behind the wall for both the non-skewed backwall and for the 30° test. However, heave greater than about 0.75 inches extended to distances of 10 to 12 feet (3.0 to 3.7 m) longitudinally behind the walls. In previous tests, surface cracking was often associated with surface heaves of approximately 0.5 to 0.75 inches (1.3 to 1.9 cm). For example, when the backfill consisted of gravel only, without embedded geotextile sheets, surface cracks were manifest at distances of 10 to 12 feet (3.0 to 3.7 m) behind the wall.

Unlike other forms of confinement (i.e. concrete wingwalls, MSE wingwalls), the geotextile reinforcement allowed the failure wedge to extend beyond the edge of the pile cap walls. Thus, the effective width of the failure wedge extended about 3 ft (0.91 m) beyond the edge of the abutment on either side, similar to an otherwise unconfined test.

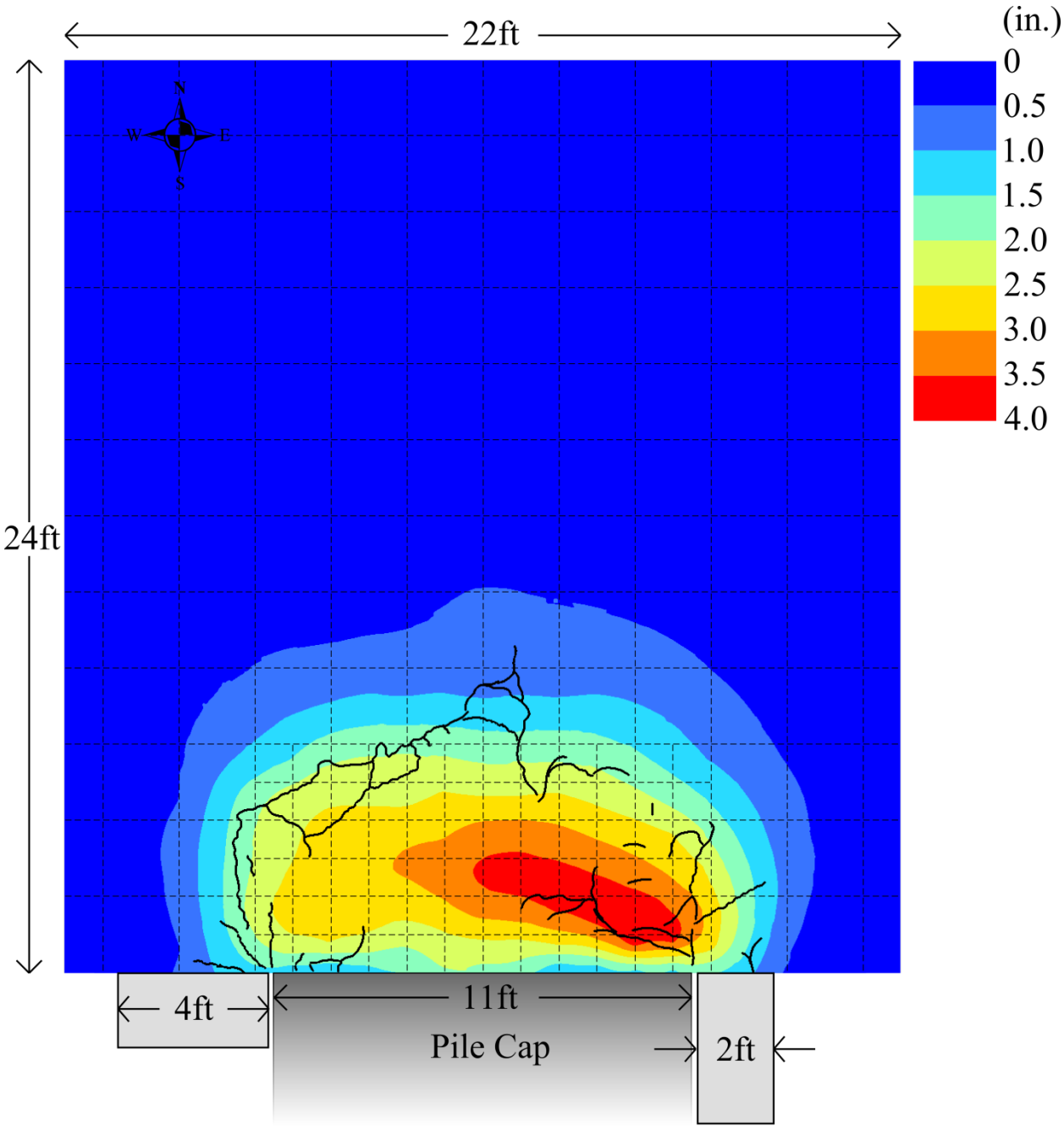

Figure 27. Heave contours (units in inches) and surface cracks at 3.74 in (9.51 cm) of longitudinal displacement (test completion) for 0° skew test (NOTE: 1 inch = 2.54 centimeters).

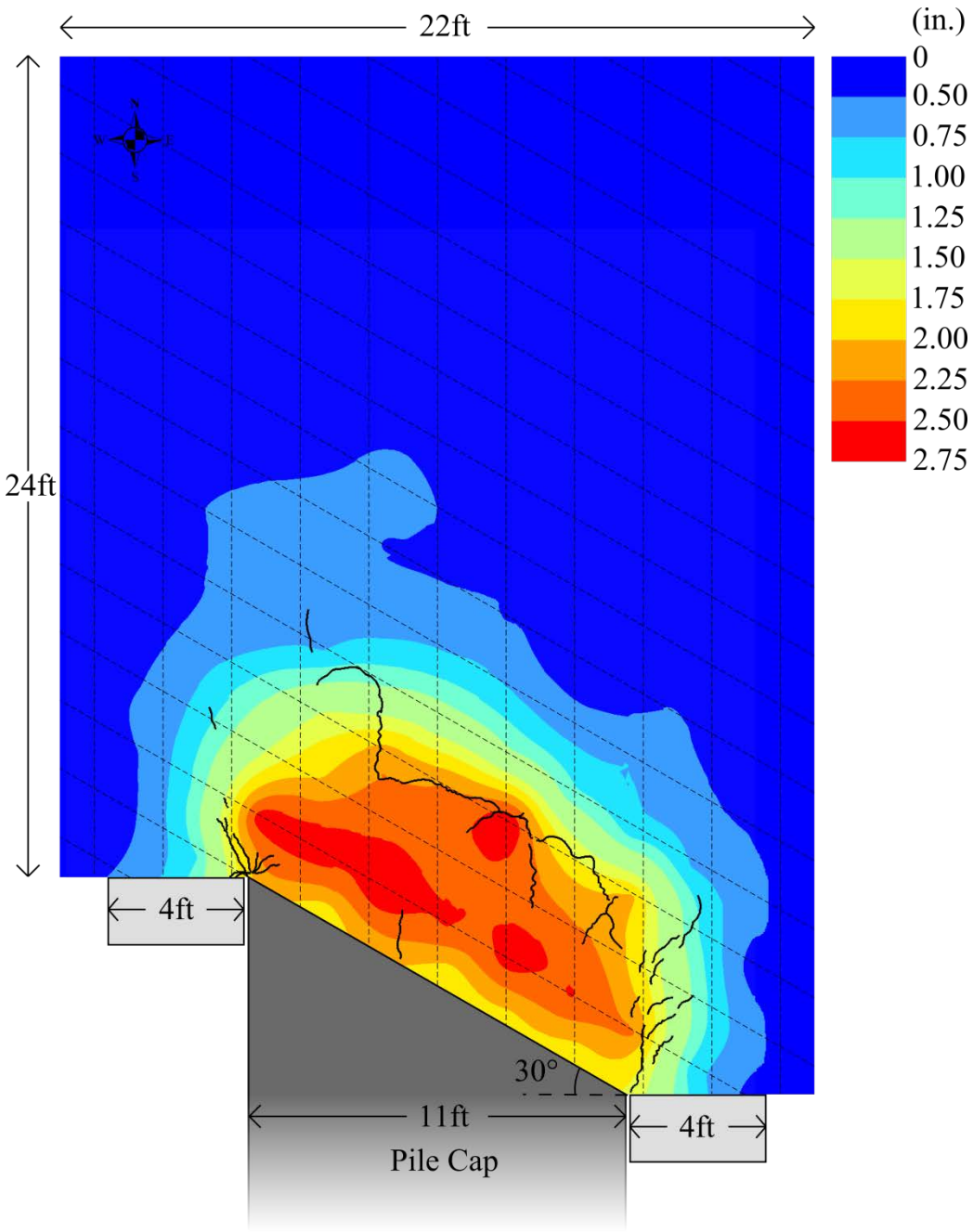

Figure 28. Heave contours (units in inches) and surface cracks at 3.0 in (7.61 cm) of longitudinal displacement (test completion) for 30° skew (NOTE 1 inch = 2.54 centimeters)

Figure 29 and Figure 30 show horizontal backfill displacements for the non-skewed and 30° skewed abutments. In contrast to the heave plots, the displacement vectors show symmetric movement on the east and west sides of the wall for the non-skewed test. Displacement vectors for both tests generally indicate longitudinal movement of the backfill with an outward component near the edges of the

backwall. However, the outward movement component is somewhat larger near the acute side of the wall for the 30º skew tests. Small variations in vector direction are typical of the similar diagrams from other tests. Displacement vector magnitudes are generally less than about 0.5 inch (1.3 cm) beyond distances of 14 to 16 ft (4.3 to 4.9 m) for both the non-skewed and 30° walls.

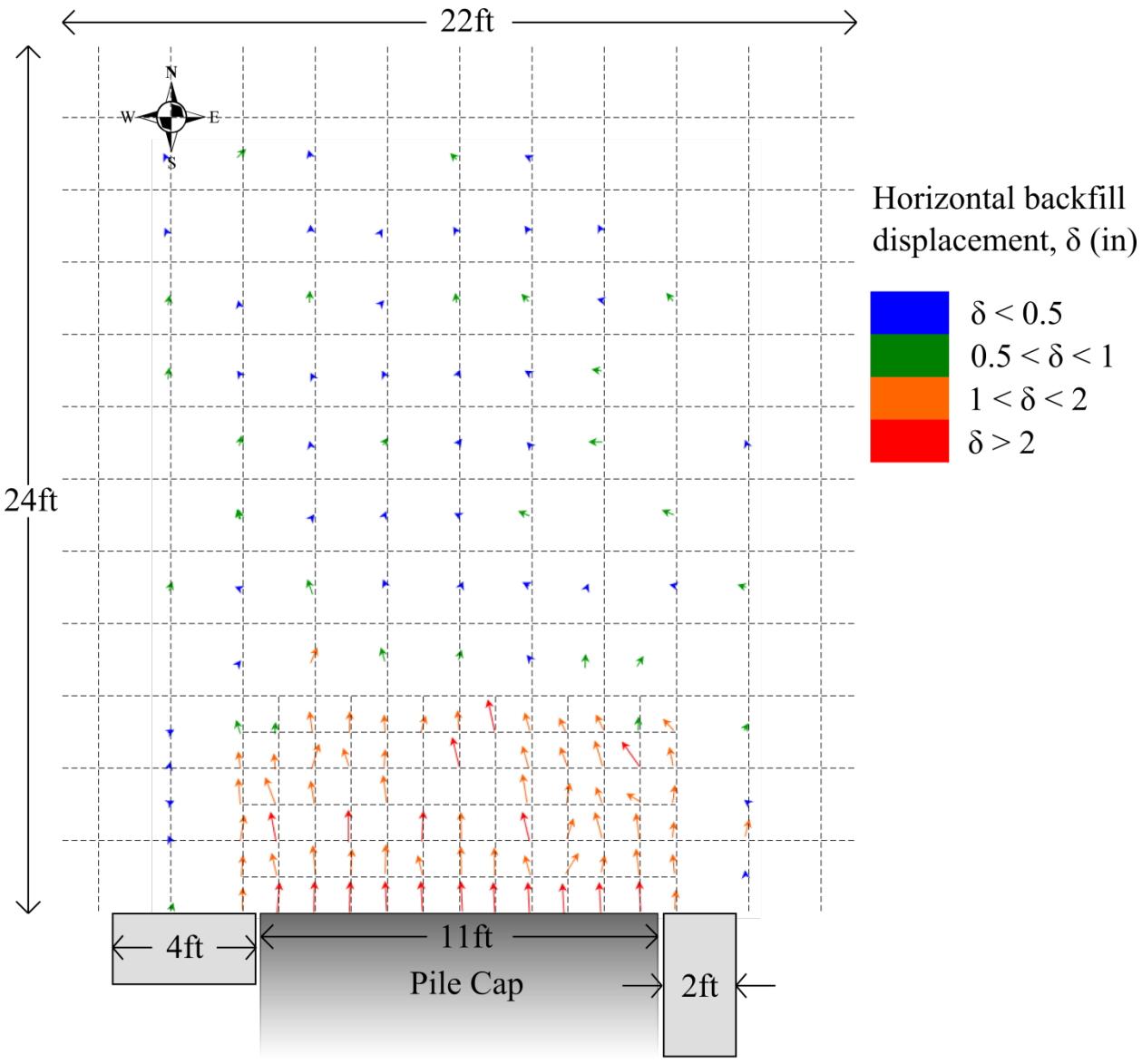

Figure 29. Soil displacement for 0° skew 3.5 ft. gravel backfill with GRS fabric at 6 in. layers.

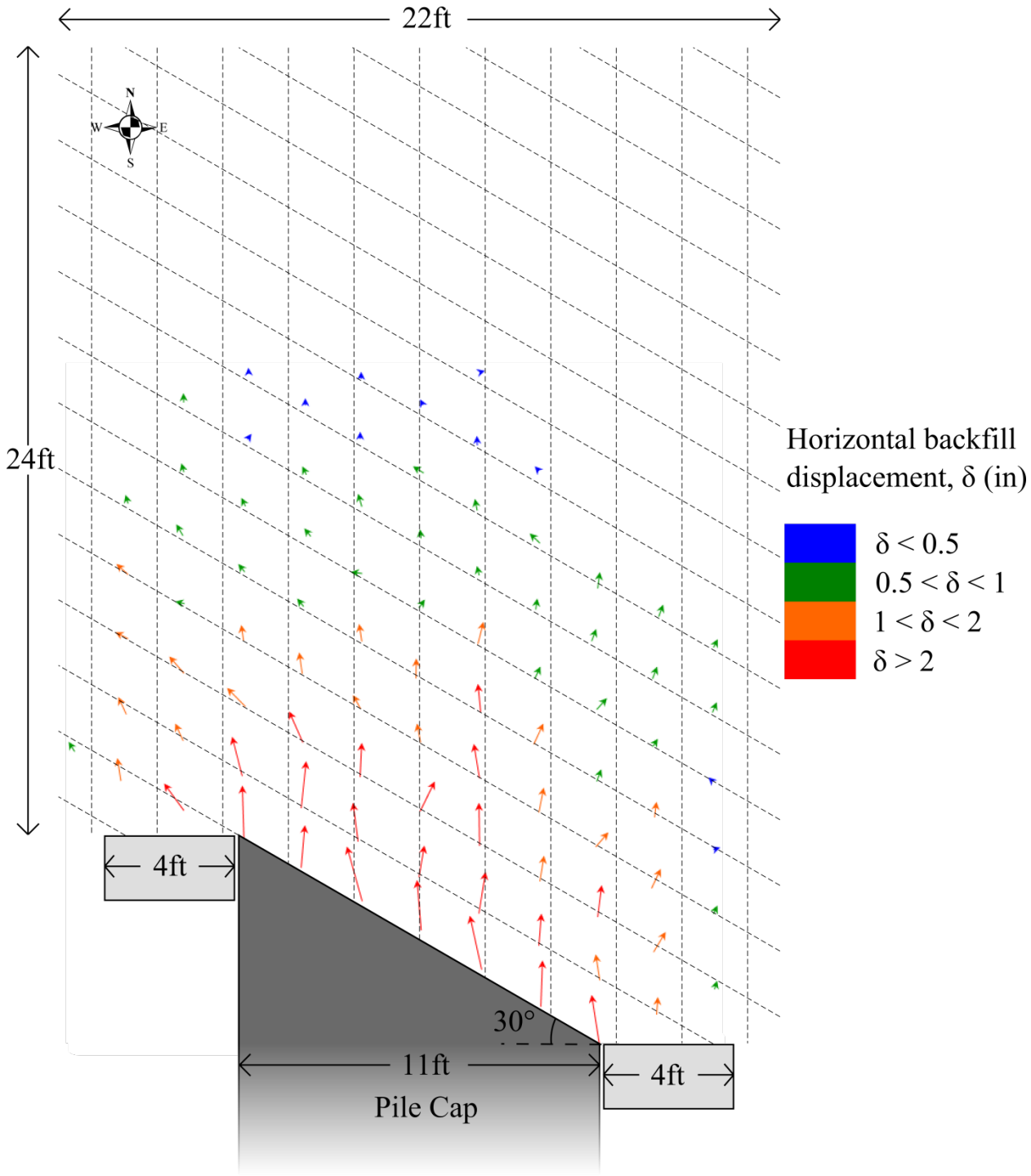

Figure 30. Soil displacement for 30° skew 3.5 ft. gravel backfill with GRS fabric at 1-ft layers.

CONCLUSIONS

1. Field tests conducted in this investigation confirm results from lab tests and numerical analyses that there is a significant reduction in peak passive force as abutment skew angle increases.
2. Although these tests involved a GRS backfill with dense sandy gravel backfill rather than a gravel backfill only, the results obtained from the field test generally verify the reduction factor versus skew equation proposed by Rollins and Jessee (2013). However, the measured reduction factor is somewhat higher than the predicted value (0.61 vs 0.50). These results, which are similar to those for the gravel backfill tests, suggest that a somewhat higher reduction factor may be appropriate for gravel backfills in comparison with sand backfills. Additional tests would be necessary to investigate this issue further and confirm that this is not simply scatter about the mean curve.
3. Although one might expect the GRS backfill to develop higher passive resistance than a similar backfill without geosynthetic layers, the resistance was actually 10 to 15% less. The increased resistance provided as the shear surface in the backfill intersected the geosynthetic layers may have been counter-balanced by lower interface friction between the concrete pile cap and the geosynthetic sheets which would lower the passive resistance. In addition, the geotextile sheets may have bent across the failure plane and had insufficient displacement or confining pressure to mobilize significant additional resistance. Additional interface friction testing and passive force analysis which is currently being undertaken will help understand this behavior.
4. The GRS backfill required significantly more movement to develop passive resistance (Approximately 0.09H) than a similar backfill without geosynthetic sheets (0.06H). In previous testing with other granular backfills, peak passive resistance was typically mobilized with normalized displacements between 0.03H and 0.06H.

ACKNOWLEDGMENTS

Funding for this study was provided by an FHWA pooled fund study supported by Departments of Transportation from the states of California, Minnesota, Montana, New York, Oregon, Utah and

Wisconsin. Utah served as the lead agency with David Stevens as the project manager. This support is gratefully acknowledged; however, the opinions, conclusions and recommendations in this paper do not necessarily represent those of the sponsoring organizations. We also express appreciation to the Salt Lake City Airport Department for providing access to the test site used in this study.

REFERENCES

AASHTO (2011). "Guide Specifications for LRFD Seismic Bridge Design." 3-106.

Apirakyorapinit, P., Mohammadi, J., and Shen, J. (2012). "Analytical Investigation of Potential Seismic Damage to a Skewed Bridge." *Practice Periodical on Structural Design and Construction*, 16(1), 5-12.

Burke Jr., M. P. (1994). "Semi-Integral Bridges: Movements and Forces." 1-7.

Caltrans (2001). "Seismic Design Criteria Version 1.2." California Department of Transportation, Sacramento, California.

Duncan, J. M., and Mokwa, R. L. (2001). "Passive Earth Pressures: Theories and Tests." *Journal of Geotechnical and Geoenvironmental Engineering, ASCE*, 127(3), 248-257.

Elnashai, A. S., Gencturk, B., Kwon, O., Al-Qadi, I. L., Hashash, Y., Roesler, J. R., Kim, S. J., Jeong, S., Dukes, J., and Valdivia, A. (2010). "The Maule (Chile) Earthquake of February 27, 2010: Consequence Assessment and Case Studies." Department of Civil and Environmental Engineering, University of Illinois at Urbana-Champaign, 190.

Lee, K. L., and Singh, A. (1971). "Relative Density and Relative Compaction." *Journal of Soil Mechanics and Foundations Design*, 97(7), 1049-1052.

Mokwa, R. L., and Duncan, J. M. (2001). "Experimental Evaluation of Lateral-Load Resistance of Pile Caps." *Journal of Geotechnical and Geoenvironmental Engineering, ASCE*, 127(2), 185-192.

Rollins, K. M., and Cole, R. T. (2006). "Cyclic Lateral Load Behavior of a Pile Cap and Backfill." *Journal of Geotechnical and Geoenvironmental Engineering, ASCE*, 132(9), 1143-1153.

Rollins, K. M., Gerber, T., Cummins, C., and Herbst, M. (2009). "Monitoring Displacement vs. Depth in Lateral Pile Load Tests with Shape Accelerometer Arrays." *Proceedings of 17th International on Soil Mechanics & Geotechnical Engineering*, 3, 2016-2019.

Rollins, K. M., Gerber, T. M., Cummins, C. R., and Pruett, J. M. (2010). "Dynamic Pressure on Abutments and Pile Caps." *Report No. UT-10.18*, B. Y. University, U. D. o. Transportation, and F. H. Administration, eds., Utah Department of Transportation, 255.

Rollins, K. M., Gerber, T. M., and Heiner, L. (2010). "Passive Force-Deflection Behavior for Abutments with MSE Confined Approach Fills." *Report No. UT-10.15*, Utah Department of Transportation.

Rollins, K. M., and Jessee, S. (2012). "Passive Force-Deflection Curves for Skewed Abutments." *Journal of Bridge Engineering*, 17(5).

Rollins, K. M., and Sparks, A. E. (2002). "Lateral Load Capacity of a Full-Scale Fixed-Head Pile Group." *Journal of Geotechnical and Geoenvironmental Engineering, ASCE*, 128(9), 711-723.

Sandford, T. C., and Elgaaly, M. (1993). "Skew Effects on Backfill Pressures at Frame Bridge Abutments." *Transportation Research Record: Journal of the Transportation Research Board*, 1-11.

Shamsabadi, A., Kapuskar, M., and Zand, A. (2006). "Three-Dimensional Nonlinear Finite-Element Soil-Abutment Structure Interaction Model for Skewed Bridges." *5th National Seismic Conference On Bridges and Highways*, FHWA, ed.San Francisco, CA, 1-10.

Shamsabadi, A., Rollins, K. M., and Kapaskur, M. (2007). "Nonlinear Soil-Abutment-Bridge Structure Interaction for Seismic Performance-Based Design." *Journal of Geotechnical and Geoenvironmental Engineering, ASCE*, 133(6), 707-720.

Steinberg, E., and Sargand, S. (2010). "Forces in Wingwalls from Thermal Expansion of Skewed Semi-Integral Bridges." *Report No. FHWA/OH-2010/16*, Prepared by Ohio University for Ohio Department of Transportation, Athens, OH, 87.

Strassburg, A. N. (2010). "Influence of Relative Compaction on Passive Resistance of Abutments with Mechanical Stabilized Earth (MSE) Wingwalls."M.S. Thesis, Brigham Young University, Provo, UT.

Unjohn, S. "Repair and Retrofit of Bridges Damaged by the 2010 Chile, Maule Earthquake." *Proc., International Symposium on Engineering Lessons Learned from the 2011 Great East Japan Earthquake*.